Spectroscopic Investigation on the Microscopic Solvation Effect on the Intramolecular Charge-Transfer Process of (*p*-Cyanophenyl)pentamethyldisilane in Supersonic Jets†

Haruki Ishikawa,* Masuyuki Sugiyama, Yoichi Shimanuki, Yuko Tajima, Wataru Setaka, Mitsuo Kira, and Naohiko Mikami*

Department of Chemistry, Graduate School of Science, Tohoku University, Aoba-ku, Sendai 980-8578, Japan

Received: May 8, 2003; In Final Form: July 19, 2003

To investigate the microscopic solvation effect on the intramolecular charge-transfer (ICT) reaction of (*p*-cyanophenyl)pentamethyldisilane (CPDS), laser-induced fluorescence and dispersed fluorescence (DF) spectra of clusters of CPDS solvated by H_2O or acetonitrile (AN) were observed in supersonic jets. In both clusters, a dual emission originating from a locally excited (LE) $\pi\pi^*$ and a charge-transfer (CT) state was observed. Two significant microscopic solvation effects were observed: an increase in the Stokes shift and an acceleration of the ICT process. The increases in the Stokes shift were found to be 1100 and 1700 cm^{-1} for CPDS−$(H_2O)_1$ and −$(AN)_1$, respectively. A trend of these clusters was related to the stabilization of the CT state by the dipole−dipole interaction with the solvent molecule. Concerning the rate of the ICT process, an unexpected result was found by lifetime measurements. The rate of the ICT process is found to be slower in the case of the CPDS−$(AN)_1$ cluster than that of the CPDS−$(H_2O)_1$ cluster, while the stabilization of the CT state is larger in the former. It was considered that this behavior reflects a reduction of a Franck−Condon overlap between the LE and the CT states, which comes from changes in the relative orientations between the LE and the CT states in the cases of these clusters.

1. Introduction

In the field of photochemistry for organic molecules of physicochemical importance, molecular vibrational dynamics in the electronic excited state is very important. It is well-known that a low-frequency vibration such as an internal rotation accelerates the intramolecular vibrational energy redistribution (IVR) and vibrational predissociation of van der Waals clusters based on extensive studies carried out by Parmenter and his group.[1] The intramolecular charge-transfer (ICT) process is another example where a low-frequency vibration plays an important role in the excited-state dynamics. Since the first report on dual fluorescence of *p*-(dimethylamino)benzonitrile (DMABN) given by Lippert,[2] a vast number of studies have been devoted to elucidating the mechanism of this process.[3] The most widely accepted model is the twisted intramolecular charge-transfer (TICT) model, where a 90° twist of the electron-donating dimethylamino group with respect to the electron-accepting aromatic ring is considered to stabilize the charge-transfer (CT) electronic state.[4] In this mechanism, the torsional vibration of the dimethylamino group plays a very important role in the ICT process. However, several mechanisms other than the TICT model still have been proposed; for example, a pseudo-Jahn−Teller interaction of two energetically close-lying ^1L_a and ^1L_b type benzenic states,[5] an in-plane bending and rehybridization at the acceptor substituent,[6] and a quinoid-type structure model.[7]

When one considers the ICT process of a molecule in condensed phases, at least two factors must be taken into account: intra- and intermolecular points of view. The former involves a deformation of the molecular structure, such as a twist of the electron-donating group with respect to the accepting one. To investigate this factor, the solvation effect must be eliminated. In solution, even though the CT state is prepared intramolecularly as a result of a large geometrical change, it is difficult to extract information about an intrinsic nature of the CT state. Thus, spectroscopic measurements in the jet-cooled isolated condition enable us to investigate characteristics of the CT state itself. Such information turns out to be a very important basis to discuss the solvation effect on the ICT process. The latter or intermolecular factor is related to solute−solvent interactions, the so-called solvation effect. In general, a CT electronic excited state is considered to be stabilized by strong electrostatic interactions between the solute and polar solvents. Since such a molecular cluster is considered to be a microscopic model of solution, a number of experimental studies have been carried out on clusters of ICT systems such as DNABN[8−12] and 9,9′-bianthryl.[13,14]

Phenylpentamethyldisilane and its derivatives are also known to exhibit ICT emission in solution.[15−23] Stabilization effects of the ICT state by substitution with an electron-accepting group as well as solvation effects have been reported.[15,16] To reveal intrinsic characteristics of the CT electronic state, we have carried out a laser spectroscopic study on jet-cooled (*p*-cyanophenyl)pentamethyldisilane (CPDS) in the previous study.[24] We have reported an observation of a dual emission of the CPDS monomer in the jet-cooled isolated condition and an experimental identification of the presence of a promoting mode for the CT state formation. The promoting mode was assigned as a torsional motion of the disilanyl group with respect to the phenyl ring. An electronic configuration of the CT state was also determined to be the (σ_{Si-Si}, $2p\pi^*$) type based on two-color resonance-enhanced two photon ionization efficiencies between the CT and LE states. Based on the electronic

* To whom correspondence should be addressed. E-mail: Haruki Ishikawa, haruki@qclhp.chem.tohoku.ac.jp; Naohiko Mikami, nmikami@qclhp.chem.tohoku.ac.jp.

† Part of the special issue "Charles S. Parmenter Festschrift".

10.1021/jp035270t CCC: $25.00
Published on Web 09/04/2003

configuration of the CT state, an accepting mode of the ICT process was assigned to be the Si−Si stretching mode rather than the torsional motion.

In the present study, laser-induced fluorescence and dispersed fluorescence spectra of solvated CPDS clusters were observed, to investigate microscopic solvation effects on the ICT process of CPDS. In addition, temporal profiles of the CT emissions were also recorded. Water (H_2O) and acetonitrile (AN) molecules were used as solvents. We discuss two important solvent effects, a stabilization of the CT state and an acceleration of the ICT process of CPDS. The rate of the ICT process is found to be slower in the case of the CPDS−$(AN)_1$ cluster than that of the CPDS−$(H_2O)_1$ cluster, while the stabilization of the CT state is larger in the former.

2. Experimental Section

In the present study, a conventional supersonic jet apparatus and a laser system were used. CPDS was synthesized by a method described in ref 16. CPDS was heated to 350 K to gain enough vapor pressure. The CPDS vapor seeded in He gas which contains a small amount of vapor of solvent molecules was supersonically expanded into a vacuum chamber through a pulsed nozzle with an orifice 0.8 mm in diameter. Concentrations of solvent molecules diluted in He were adjusted so that sharp bands of solvated CPDS clusters clearly appeared in the LIF spectra. A frequency-doubled output of a tunable dye laser (LAS LDL 20202) pumped by a Nd:YAG laser (Continuum Surelite II) was used for the excitation of the solvated CPDS clusters. The laser light irradiated the jet 10−15 mm downstream from the nozzle orifice. The fluorescence was collected with a lens placed at a right angle to both the jet and the laser beam and was detected by a photomultiplier tube (PMT) (Hamamatsu 1P28). The signal was integrated by a boxcar averager (EG&G Par 4420) and processed by a microcomputer. When dispersed fluorescence (DF) spectra were measured, a small monochromator (Nikon P250) was placed in front of the photomultiplier tube. In addition, a total or undispersed fluorescence was collected simultaneously from the opposite side to the DF measuring system. This fluorescence intensity was used to compensate fluctuations of laser intensity and a long-time change in a nozzle operation condition. In this case, a wide slit width of the monochromator was set to 1 mm. In the measurement of fluorescence time profiles, a fast-response PMT (Hamamatsu R1564U-06) of the 0.1-ns response was used. The monochromator was set in front of the PMT to discriminate the CT or the LE emission component. The time profiles of the emission were recorded by a digital oscilloscope (LeCroy 9354AL) operating in a random interleaved mode. Fundamental outputs of laser wavelengths were calibrated by simultaneously recorded LIF spectra of molecular iodine.[25]

3. Results and Discussion

A. LIF Spectra of Solvated CPDS Clusters. Figure 1 shows LIF spectra of solvated CPDS clusters observed in the present study. A LIF spectrum displayed in the top panel was measured without adding acetonitrile to the sample. 0_0^0 band of CPDS monomer appears at 35 518.8 cm^{-1} accompanying a low-frequency progression of a 25-cm^{-1} interval. This low-frequency vibration was assigned to be a torsional motion (τ) of the disilanyl group with respect to the phenyl ring in our previous study.[24] Similar low-frequency progressions starting at 35 456.5 and 35 394.3 cm^{-1} were assigned to the bands of CPDS−$(H_2O)_n$, $n = 1$ and 2 clusters, respectively. The number of water molecules was determined by a resonance-enhanced multiphoton ionization (REMPI) measurement. A small amount of water vapor which contaminated the sample compartment was found to be sufficient to provide an abundance of CPDS−$(H_2O)_n$ clusters. The red shifts of the 0_0^0 bands of CPDS−$(H_2O)_{n=1,2}$ clusters measured from that of the monomer were found to be 62.5 and 124.7 cm^{-1} for the $n = 1$ and 2 clusters, respectively.

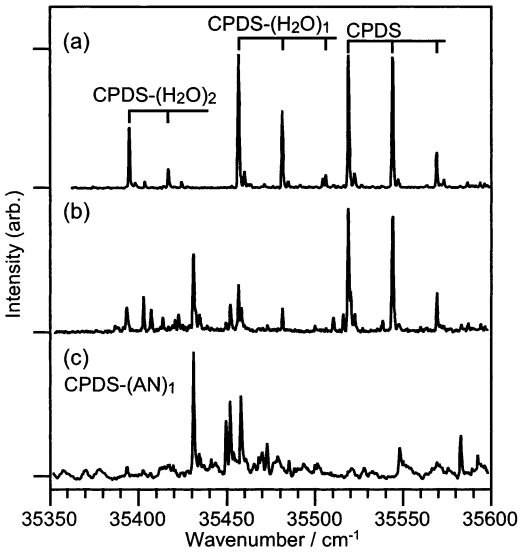

Figure 1. LIF spectra of jet-cooled CPDS and its solvated clusters. Recorded without (a) and with (b) acetonitrile in the sample. Mass-selected REMPI spectrum which monitored the mass of CPDS−$(AN)_1$ is shown in trace (c).

TABLE 1: Wavenumbers of the 0_0^0 Band ($\tilde{\nu}_0$) and Intensity Maximum of the CT Emission ($\tilde{\nu}_{CT}$), and the Stokes Shift ($\tilde{\nu}_{Stokes}$) of CPDS and Its Solvated Clusters[a]

	$\tilde{\nu}_0$	$\Delta\tilde{\nu}_0$	$\tilde{\nu}_{CT}$[b]	$\tilde{\nu}_{Stokes}$[b]	$\Delta\tilde{\nu}_{Stokes}$[b]
CPDS	35 518.8		28 700	6800	
CPDS−$(H_2O)_1$	35 456.5	−62.3	27 550	7900	1100
CPDS−$(AN)_1$	35 430.9	−87.9	26 900	8500	1700

[a] Shift of $\tilde{\nu}_0$ and $\tilde{\nu}_{Stokes}$ compared with those of the monomer ($\Delta\tilde{\nu}_0$,$\Delta\tilde{\nu}_{Stokes}$) are also listed. All the values are in unit of cm^{-1}. [b] Uncertainty in the DF spectra was about 50 cm^{-1}.

Figure 1b shows a LIF spectrum recorded when acetonitrile (AN) molecules were diluted in He carrier gas. A strong peak at 35 430.9 cm^{-1} was assigned to the 0_0^0 band of the CPDS−$(AN)_1$ cluster. It was confirmed by a REMPI spectrum, which monitored the mass of CPDS−$(AN)_1$ (274 amu), shown in Figure 1c. The amount of red shift of the 0_0^0 band measured from that of the CPDS monomer (87.9 cm^{-1}) is larger than that of the CPDS−$(H_2O)_1$ cluster. Spectral carriers of bands appearing near 35 400 cm^{-1} are assigned as CPDS−$(AN)_2$ clusters. Details concerning these bands will be reported in a forthcoming paper.[26] In Table 1, the wavenumbers of the 0_0^0 bands ($\tilde{\nu}_0$) and the amounts of their red shift ($\Delta\tilde{\nu}_0$) for both clusters compared with that of the monomer are summarized.

B. DF Spectra of Solvated CPDS Clusters. Dispersed fluorescence (DF) spectra from the 0_0^0 band of each cluster are shown in Figure 2. For comparison, a DF spectrum from the τ^2 level of the monomer is also represented in Figure 2a. It is clearly seen that strong structureless broad emissions appear in all the spectra. The broad part appearing below 32 000 cm^{-1} is due to the CT emission from the ICT state. On the other hand, the structured part above 32 000 cm^{-1} is called the LE emission from the locally excited state. Wavenumbers of intensity maxima of the CT emissions ($\tilde{\nu}_{CT}$) were evaluated by fitting the spectra with Gaussian functions. The values of $\tilde{\nu}_{CT}$ and Stokes shifts

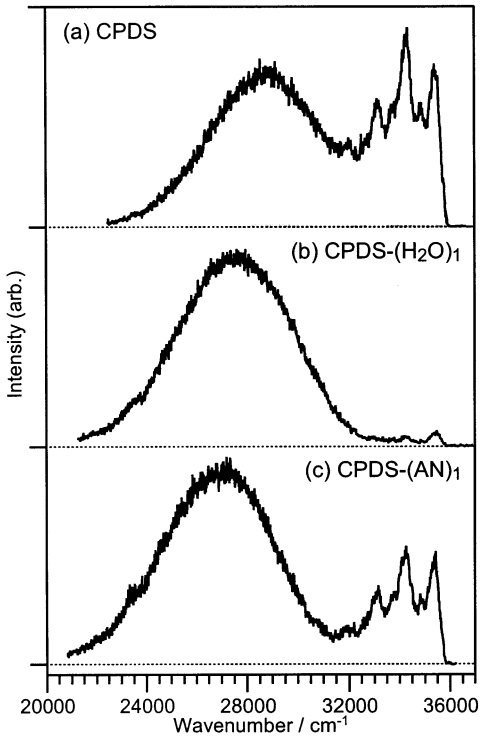

Figure 2. Dispersed fluorescence spectra of CPDS and its solvated clusters. (a) CPDS monomer excited at the τ_0^2 band. (b) CPDS−$(H_2O)_1$ cluster excited at the 0_0^0 band. (c) CPDS−$(AN)_1$ cluster excited at the 0_0^0 band.

($\tilde{\nu}_{Stokes} = \tilde{\nu}_0 - \tilde{\nu}_{CT}$) of these clusters are also summarized in Table 1. An attachment of a single H_2O molecule provides an increase in the Stokes shift ($\Delta\tilde{\nu}_{Stokes}$) of 1100 cm^{-1} compared with that of the monomer, whereas this value is 1700 cm^{-1} for the case of AN. These increases in the Stokes shift due to the clustering of a solvent molecule are one of the clear features of the microscopic solvation effect. A trend of the increases in the Stokes-shift observed in the present study is very reasonable, since the CT state is more stabilized by a solvent having a larger dipole moment. The dipole moments are 1.854 and 3.924 D for H_2O and AN, respectively.[27]

In the case of the CPDS−$(H_2O)_1$ cluster, a relative intensity of the LE emission decreases very much compared with that of the monomer. This indicates an acceleration of the ICT process due to the solvation. CPDS clusters solvated with Ar or other solvent molecules were found to exhibit similar results to the CPDS−(H_2O) clusters in our preliminary experiments.[26] However, LE emission with an appreciable intensity was observed in the case of the CPDS−$(AN)_1$ cluster as shown in Figure 2c. This was a rather unexpected result. Since the relative intensity ratio between the LE and CT emissions reflects the rate of the ICT process, it was indicated that the ICT process is less accelerated in the case of the CPDS−$(AN)_1$ cluster compared in the CPDS−$(H_2O)_1$ cluster. To examine the rate of the ICT process, lifetime measurements were carried out.

C. Temporal Profiles of the CT States of Solvated CPDS Clusters. Figure 3 shows time profiles of the LE and CT emission from the vibrational ground level of the CPDS−$(AN)_1$ cluster in the LE excited state. In each trace, a response function of our apparatus, which measured as a time profile of a scattered light, is also displayed. The width of the response function was mainly determined by the temporal width of the laser pulses used in the present study. For comparison, the time profile of the CT emission of the CPDS−$(H_2O)_1$ cluster is also shown in Figure 3c. A time profile of the LE state of the water complex

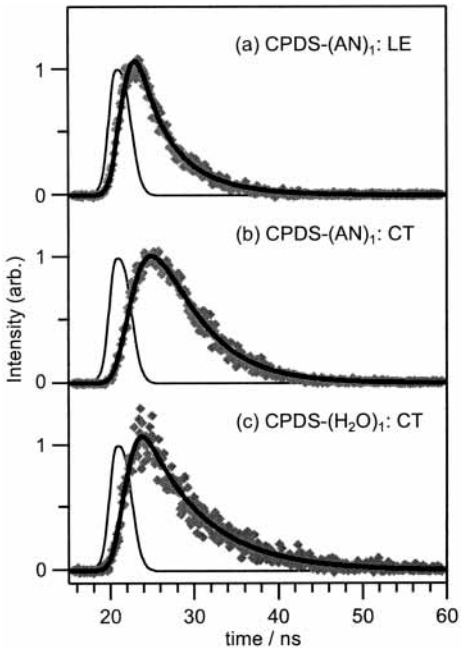

Figure 3. Temporal profiles of (a) the LE and (b) the CT states of CPDS−$(AN)_1$ and (c) the CT state of CPDS−$(H_2O)_1$ clusters. All the profiles were measured at the 0_0^0 band excitation. Observed data are represented as filled diamonds, whereas thick solid lines indicate simulated profiles. Thin solid lines indicate response functions of our system.

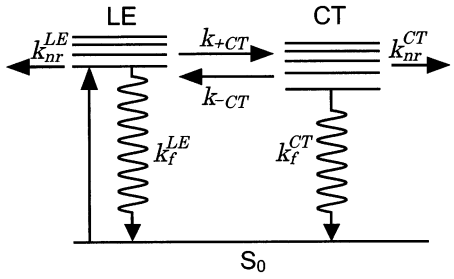

Figure 4. Two-states model of the ICT process. Rate constants denoted in the figure are defined in the text.

could not be observed, since the LE emission intensity was too low. As seen in Figure 3b,c, both of the CT emissions of the CPDS−$(AN)_1$ and −$(H_2O)_1$ clusters exhibit a profile with rise and decay components. Apparently, the rise rate of the CPDS−$(AN)_1$ is slower than that of the CPDS−$(H_2O)_1$.

The time profiles were analyzed assuming the kinetic model schematically represented in Figure 4. In this model, temporal profiles of the LE and the CT state populations are expressed as follows.

$$I_{LE}(t) = \left\{\frac{k_1 - \lambda_2}{\lambda_1 - \lambda_2}\exp(-\lambda_1 t) + \frac{\lambda_1 - k_1}{\lambda_1 - \lambda_2}\exp(-\lambda_2 t)\right\} I_{LE}^0 = A_1 \exp(-\lambda_1 t) + A_2 \exp(-\lambda_2 t) \quad (1)$$

$$I_{CT}(t) = \frac{k_{+CT}}{\lambda_1 - \lambda_2}\{\exp(-\lambda_2 t) - \exp(-\lambda_1 t)\} I_{LE}^0 = A_{CT}\{\exp(-\lambda_2 t) - \exp(-\lambda_1 t)\} \quad (2)$$

where I_{LE}^0 is an initial population of the LE state in arbitrary units

$$\lambda_{1,2} = \frac{1}{2}(k_1 + k_2) \pm \frac{1}{2}\{(k_1 - k_2)^2 + 4k_{+CT}k_{-CT}\}^{1/2} \quad (3)$$

TABLE 2: Parameters Obtained in the Temporal Profile Analysis for Each Species[a]

	state	$(1/\lambda_1)$, ns	$(1/\lambda_2)$, ns
CPDS	CT	3.9	15.0
CPDS−$(H_2O)_1$	CT	0.6	7.1
CPDS−$(AN)_1$	CT	2.2	5.1
CPDS−$(AN)_1$	LE[c]	2.2[b]	5.1[b]

[a] The definition of each parameter is described in the text. [b] Fixed in the fit. [c] $A_1/A_2 = 0.674$.

and

$$k_1 = k_f^{LE} + k_{nr}^{LE} + k_{+CT}, \quad k_2 = k_f^{CT} + k_{nr}^{CT} + k_{-CT} \qquad (4)$$

Here, $k_f^{LE(CT)}$ and $k_{nr}^{LE(CT)}$ are rate constants for the fluorescence and the nonradiative decay in the LE(CT) state, respectively. The rate constants of the forward and backward CT processes are k_{+CT} and k_{-CT}, respectively. All the rate constants, k and λ, are in units of s^{-1}. The time profiles of the CT emission of AN and H_2O clusters displayed in parts b and c of Figure 3, respectively, were analyzed by least-squares fits based on eq 2. The time profiles of the CT emission were well-reproduced as shown in the figure. Parameters obtained by the fits were listed in Table 2. A time profile of the CT emission from the 0° level of the CPDS monomer was also analyzed in the same manner. Parameters obtained by the fit agreed well with those obtained by a pump−probe measurement reported in ref 24. The rise and decay time constants $(1/\lambda_{1,2})$ of the CT state of both solvated clusters are smaller compared with those of the monomer. The decrease in the rise time constant indicates the acceleration of the ICT process by the solvation, while the decrease in the decay constant is considered to be due to an opening of a nonradiative decay process such as dissociation.

When the two-states model is applicable, the time profile of the LE state should be expressed by eq 1. In general, the least-squares fit of such a profile becomes difficult or less plausible when values of two exponents are close in order due to a numerical instability in the fitting procedure. Thus, only two preexponential factors were fitted, while two exponents were fixed to the values obtained in the fit of the CT emission, in the analysis of the LE emission of the CPDS−$(AN)_1$ cluster. The result of the fit was well-acceptable. This means that the ICT process of the CPDS−$(AN)_1$ can be described by the two-state model as expressed in Figure 4.

The analysis of the temporal profiles of the CT states of both clusters clearly showed that the effective rate of the CT state formation of the CPDS−$(AN)_1$ cluster is much slower than that of the CPDS−$(H_2O)_1$ cluster. This unexpected behavior will be discussed below.

D. DFT Calculation of the Structure of Solvated CPDS Clusters. Structures of the solvated CPDS clusters in their S_0 state were elucidated by density fuctional theory (DFT) calculations at the B3LYP/6-31G(d,p) level. The Gaussian 98 program package[28] was used in the calculation. Figure 5 shows optimized structures of both clusters. In both cases, the solvent molecule, H_2O or AN, is attached near the CN group of CPDS. The local structures are very similar to those of benzonitrile clusters.[29,30] In the case of the CPDS−$(H_2O)_1$ cluster, the water molecule is attached by the hydrogen bonding between the π-electron of the CN group and the hydrogen of water. In addition to the hydrogen bonding, there should be an appreciable contribution of the dipole−dipole interaction. On the other hand, the main contribution of the cluster formation is the dipole−dipole interaction in the case of CPDS−$(AN)_1$. Relative orientation between the two CN groups is not strictly parallel. This is considered to be due to the electrostatic interaction between the π-electron and hydrogen atoms of the phenyl and methyl groups. Binding energies of these clusters were calculated to be 1360 and 1410 cm^{-1} for the CPDS−$(H_2O)_1$ and the CPDS−$(AN)_1$ clusters, respectively. A basis-set superposition error was corrected. Thus, the stabilization of the S_0 state by the solvation was found to be nearly the same for these clusters, though the origins of the intermolecular forces are different.

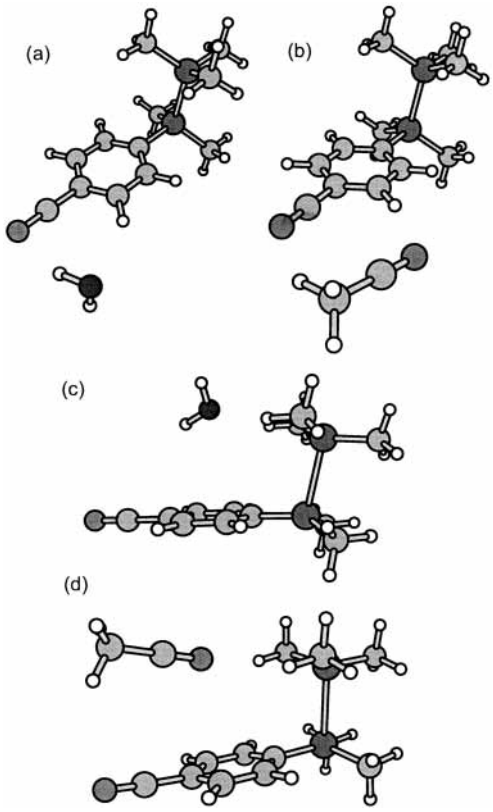

Figure 5. Optimized structures of solvated CPDS clusters obtained by DFT calculations at the B3LYP/6-31G(d,p) level. (a) CPDS−$(H_2O)_1$ in S_0, (b) CPDS−$(AN)_1$ in S_0, (c) CPDS−$(H_2O)_1$ in D_0, and (d) CPDS−$(AN)_1$ in D_0. See details in the text.

The present calculations are limited to the S_0 state. However, in both the clusters, the relative orientation between the CPDS and solvent molecules in the LE state should be very close to that in the S_0 state. The similarity is rationalized from the LIF and REMPI spectra shown in Figure 1a and c, in which the intensity of the origin band of each cluster is the strongest among the vibronic bands. The large FC factor of the origin band represents that the structural change upon the excitation should be small.

The relative orientation of the solvent molecule in the CT state is one of the most important factors in understanding the ICT process. In the previous study, the result of the two-color REMPI spectroscopy indicated similarities in the electronic configuration and structure between the CT and the D_0 states.[24] The electronic configuration of the D_0 state was found to be of a σ_{Si-Si}^{-1} type, where an electron in the σ_{Si-Si} orbital is eliminated upon ionization. Based on these facts, we have determined the electronic configuration of the CT state to be $\sigma_{Si-Si}\pi^*$ one. Since the CT state has a positive charge at the disilanyl group, its charge distribution should be very different from those of the S_0 and the LE states. Thus, the relative orientations of the solvents in the CT state should also be different from those in the S_0 and the LE states. However, it is difficult to determine the relative orientation of the solvents

theoretically, since it is difficult to carry out such a calculation on the CT electronic state. Instead, DFT calculations of the cationic (D_0) state were carried out for the clusters investigated here. Since the D_0 state also has a positive charge at the disilanyl group like the CT state, its charge distribution should be more similar to that of the CT state compared with the S_0 and the LE states. Thus, the DFT calculations on the D_0 state should provide us with some insights in considering the orientation of solvents in the CT state.

In both clusters, the structures presented in Figure 5a,b are found to be the global minimum of the S_0 state for each cluster. Another local minimum was not obtained either both cluster. In the case of the D_0 state, a local minimum was found for the CPDS$-(H_2O)_1$ cluster. The water molecule is located above the phenyl ring as shown in Figure 5c. In this structure, the water molecule lies in the plane which involves two silicon atoms of the disilanyl group and is perpendicular to the phenyl ring. The oxygen atom is heading to the disilanyl group, which is positively charged. This structure lies higher (290 cm^{-1}) in energy than in the structure similar to that shown in Figure 5a. On the other hand, the structure shown in Figure 5d was found to be the global minimum and the structure similar to that shown in Figure 5b was a local minimum in the case of CPDS$-(AN)_1$. In the structure shown in Figure 5d, the molecular axis of AN lies in the plane which involves two silicon atoms of the disilanyl group and is perpendicular to the phenyl ring. The energy difference between these structures is 270 cm^{-1}.

The possibility of the reorientation of the solvents was considered based on these results. In the case of CPDS$-(H_2O)_1$, it would be less possible for the reorientation of H_2O molecule to take place, since the H_2O molecule is tightly bound by the hydrogen bond. On the contrary, a possibility of the reorientation of AN molecule during the ICT process was suggested in the case of the CPDS$-(AN)_1$ cluster.

E. Microscopic Solvation Effects on the ICT Process of CPDS. As mentioned above, two significant effects of the microscopic solvation were found in the present study: the stabilization of the CT state and the acceleration of the ICT process.

In general, an increase in the Stokes shift reflects a stabilization of the CT state by solvation. The increase in the Stokes shift indicates a difference in amount of the stabilization between the CT and the S_0 states. The DFT calculations provide an estimation of the stabilization energy of the S_0 state of CPDS$-(H_2O)_1$ and $-(AN)_1$ to be about 1400 cm^{-1} for both clusters. Thus, the difference in the Stokes shift between these clusters comes from the difference in the stabilization of the CT states. Thus, our results simply indicate that the CT state of CPDS is more stabilized by the attachment of AN than H_2O. This trend is quite understandable since it is one of the features of the ICT process that the CT state is much stabilized by more polar solvent.

The relative intensity of the CT emission compared with that of the LE emission of both clusters, and the results of the temporary profile measurements indicated that the ICT process is accelerated by the interaction with a solvent molecule. However, it was rather unexpected that the rate of the ICT process of the CPDS$-(AN)_1$ cluster is slower than that of CPDS$-(H_2O)_1$. In general, the rate of the ICT process is determined by the amount of the FC overlap between the LE and the CT states potential surfaces. Thus, the FC overlap should be smaller in the case of the AN cluster compared with that of the water cluster. The FC overlap consists of intramolecular and intermolecular factors. The former represents the structural change of the CPDS molecule in the ICT process, whereas the latter is related to the reorientation of the solvent molecules. Since the former or intramolecular structural change is considered to be nearly the same between these clusters, the difference should come from the intermolecular factor. As discussed in the above section, there is a large possibility of the solvent reorientation in the case of AN cluster but a small possibiltiy for the H_2O cluster. This difference should be reflected as a large difference in the FC overlap between the LE and the CT states, that is, the change in the ICT rate.

The differences in the physical properties between AN and H_2O are the capability of hydrogen bonding and the dipole moments. A competition between the dipole−dipole interaction and the hydrogen bonding in stabilizing the energy of total systems should make a difference in the probability of the reorientation of the solvents in these clusters. To elucidate the details of the ICT process, it is necessary to measure the ICT rates of the other solvated CPDS clusters.

4. Concluding Remarks

In the present study, the microscopic solvation effects on the ICT process of (*p*-cyanophenyl)pentamethyldisilane were investigated. The two significant solvation effects were observed even in the case of 1:1 solvated clusters. The stabilization of the CT state was indicated by the increase of the Stokes shift in the DF spectrum. The amount of the stabilization in energy was related to the dipole−dipole interaction by the solvent. The most significant finding was the inverse relation between the stabilization of the ICT state and the acceleration of the ICT process compared between the cases of CPDS$-(H_2O)_1$ and $-(AN)_1$ clusters. This behavior was interpreted as a result of the difference in the FC overlap between the LE and the CT states, which indicates a possibility of the reorientation of the solvent molecules in the ICT process. To elucidate the details of the ICT process, we are carrying out measurements on clusters with other solvents and also on higher clusters.

References and Notes

(1) For example: (a) Timbers, P. J.; Parmenter, C. S.; Moss, D. B. *J. Chem. Phys.* **1994**, *100*, 1028. (b) Zhao, Z.-Q.; Parmenter, C. S. *Ber. Bunsen-Ges. Phys. Chem.* **1995**, *99*, 536.

(2) (a) Lippert, E. *Z. Naturforsch.* **1955**, *10a*, 541. (b) Lippert, E.; Lüder, W.; Boos, H. In *Advances in Molecular Spectroscopy*, Mangini, A., Ed.; Pergamon: New York, 1962; p 443.

(3) For recent reviews, see: (a) Rettig, W. *Angew. Chem., Int. Ed. Engl.* **1986**, *25*, 971. (b) Bhattacharyya, K.; Chowdhury, M. *Chem. Rev.* **1993**, *93*, 507.

(4) (a) Rotkiewicz, K.; Grellmann, K. H.; Grabowski, Z. R. *Chem. Phys. Lett.* **1973**, *19*, 315. (b) Grabowski, Z. R.; Rotkiewicz, K.; Siemiarczuk, A.; Cowley, D. J.; Baumann, W. *Nouv. J. Chem.* **1979**, *3*, 443.

(5) (a) Zachariasse, K. A.; Harr, T.; Hebecker, A.; Leinhos, U.; Kühnle, W. *Pure Appl. Chem.* **1993**, *65*, 1745. (b) Rettig, W.; Bliss, B.; Dirnberger, K. *Chem. Phys. Lett.* **1999**, *305*, 8.

(6) Sobolewski, A. L.; Domcke, W. *Chem. Phys. Lett.* **1996**, *259*, 119.

(7) Warren, J. A.; Bernstein, E. R.; Seeman, J. I. *J. Chem. Phys.* **1988**, *88*, 871.

(8) Peng, L. W.; Dantus, M.; Zewail, A. H.; Kemniz, K.; Hicks, J. M.; Eisenthal, K. B. *J. Phys. Chem.* **1987**, *91*, 6162.

(9) Howell, R.; Petek, H.; Phillips, D.; Yoshihara, K. *Chem. Phys. Lett.* **1991**, *183*, 249.

(10) Shang, Q.; Bernstein, E. R. *J. Chem. Phys.* **1992**, *97*, 60.

(11) Howell, R.; Phillips, D.; Petek, H.; Yoshihara, K. *Chem. Phys.* **1994**, *188*, 303.

(12) Howell, R.; Jones, A. C.; Taylor, A. G.; Phillips, D. *Chem. Phys. Lett.* **1989**, *163*, 282.

(13) Honma, K.; Arita, K.; Yamasaki, K.; Kajimoto, O. *J. Chem. Phys.* **1991**, *94*, 3496.

(14) Honma, K.; Kajimoto, O. *J. Chem. Phys.* **1994**, *101*, 1752.

(15) Sakurai, H.; Sugiyama, H.; Kira, M. *J. Phys. Chem.* **1990**, *94*, 1837.

(16) Kira, M.; Miyazawa, T.; Sugiyama, H.; Yamaguchi, M.; Sakurai, H. *J. Am. Chem. Soc.* **1993**, *115*, 3116.

(17) Kira, M.; Miyazawa, T. In *The chemistry of organic silicon compounds*, Rappoport, Z.; Apeloig, Y., Eds.; John Wiley & Sons: 1998; Vol. 2, Chapter 22.

(18) Shizuka, H.; Obuchi, H.; Ishikawa, M.; Kumada, M. *J. Chem. Soc., Chem. Commun.* **1981**, 405.

(19) Shizuka, H.; Sato, Y.; Ishikawa, M.; Kumada, M. *J. Chem. Soc., Chem. Commun.* **1982**, 439.

(20) Shizuka, H.; Sato, Y.; Ueki, Y.; Ishikawa, M.; Kumada, M. *J. Chem. Soc., Faraday Trans. 1* **1984**, *80*, 341.

(21) Shizuka, H.; Obuchi, H.; Ishikawa, M.; Kumada, M. *J. Chem. Soc., Faraday Trans. 1* **1984**, *80*, 383.

(22) Shizuka, H.; Okazaki, K.; Tanaka, M.; Ishikawa, M.; Sumitani, M.; Yoshihara, K. *Chem. Phys. Lett.* **1985** *113*, 89.

(23) Hiratsuka, H.; Mori, Y.; Ishikawa, M.; Okazaki, K.; Shizuka, H. *J. Chem. Soc., Faraday Trans. 2* **1985**, *81*, 1665.

(24) (a)Tajima, Y.; Ishikawa, H.; Miyazawa, T.; Kira, M.; Mikami, N. *J. Am. Chem. Soc.* **1779**, *119*, 7400. (b) Ishikawa, H.; Shimanuki, Y.; Sugiyama, M.; Tajima, Y.; Kira, M.; Mikami, N. *J. Am. Chem. Soc.* **2002**, *124*, 2002.

(25) Gerstenkorn, S.; Luc, P. *Atlas du Spectre de la Molecule de l'Iode entre 14800−20000 cm*$^{-1}$; Editions du CNRS: Paris, 1978.

(26) Ishikawa, H.; Shimanuki, Y.; Sugiyama, M.; Setaka, W.; Kira, M.; Mikami, N., manuscript in preparation.

(27) Lide, D. R. *CRC Handbook of Chemistry and Physics*, 74th ed.; CRC Press: Boca Raton, FL, 1993.

(28) Frisch, M. J.; Trucks, G. W.; Schlegel, H. B.; Scuseria, G. E.; Robb, M. A.; Cheeseman, J. R.; Zakrzewski, V. G.; Montgomery, J. A., Jr.; Stratmann, R. E.; Burant, J. C.; Dapprich, S.; Millam, J. M.; Daniels, A. D.; Kudin, K. N.; Strain, M. C.; Farkas, O.; Tomasi, J.; Barone, V.; Cossi, M.; Cammi, R.; Mennucci, B.; Pomelli, C.; Adamo, C.; Clifford, S.; Ochterski, J.; Petersson, G. A.; Ayala, P. Y.; Cui, Q.; Morokuma, K.; Malick, D. K.; Rabuck, A. D.; Raghavachari, K.; Foresman, J. B.; Cioslowski, J.; Ortiz, J. V.; Baboul, A. G.; Stefanov, B. B.; Liu, G.; Liashenko, A.; Piskorz, P.; Komaromi, I.; Gomperts, R.; Martin, R. L.; Fox, D. J.; Keith, T.; Al-Laham, M. A.; Peng, C. Y.; Nanayakkara, A.; Gonzalez, C.; Challacombe, M.; Gill, P. M. W.; Johnson, B.; Chen, W.; Wong, M. W.; Andres, J. L.; Gonzalez, C.; Head-Gordon, M.; Replogle, E. S.; Pople, J. A. Gaussian 98 (Revision A.7); Gaussian, Inc.: Pittsburgh, PA, 1998.

(29) Ishikawa, S.; Ebata, T.; Mikami, N. *J. Chem. Phys.* **1999**, *110*, 9504.

(30) Yamamoto, Y.; Ishikawa, S.; Ebata, T.; Mikami, N. J. *Raman Spectrosc.* **2000**, *31*, 295.